This is the accepted manuscript (postprint) of the following article:
N. Mosafajahanabad, M. Alizadeh, E. Salahinejad, *Accumulative roll bonding fabrication, tensile and corrosion characterization of Zn/Al multilayered composites*, Archives of Civil and Mechanical Engineering, 22 (2022) 191.
https://doi.org/10.1007/s43452-022-00521-6

Accumulative roll bonding fabrication, tensile and corrosion characterization of Zn/Al multilayered composites

Nasim Mosafajahanabad [1] · Morteza Alizadeh [1,*] · Erfan Salahinejad [2]

[1] *Department of Materials Science and Engineering, Shiraz University of Technology, Modarres Blvd., Shiraz 71557-13876, Iran*

[2] *Faculty of Materials Science and Engineering, K. N. Toosi University of Technology, Tehran, Iran*

[3]

* Corresponding author: Morteza Alizadeh: Alizadeh@sutech.ac.ir

Abstract

In the present work, accumulative roll bonding (ARB) processing and characteristics of Zn/6 wt% Al multilayered composite sheets were investigated for the first time. The structure of the fabricated composites was evaluated by X-ray diffraction (XRD) and scanning electron microscopy (SEM). Tensile testing and fractography were used to assess the strength and elongation of the composites. The corrosion behavior of the fabricated samples was also investigated by potentiodynamic polarization and electrochemical impedance spectroscopic tests in the 3.5 wt% NaCl solution. Despite the evolution of atomic intermixing at the interface of the layers and grain refinement, the tensile strength and elongation of the composites were reduced by increasing ARB cycles due to the domination of plastic instability introduced by the ARB process. In addition, an initial increase until the third ARB cycle followed by

This is the accepted manuscript (postprint) of the following article:
N. Mosafajahanabad, M. Alizadeh, E. Salahinejad, *Accumulative roll bonding fabrication, tensile and corrosion characterization of Zn/Al multilayered composites*, Archives of Civil and Mechanical Engineering, 22 (2022) 191.
https://doi.org/10.1007/s43452-022-00521-6

decrease in the corrosion tendency of the composites was found by progression of the ARB process, which was attributed to a compromise between the levels of structural defects and homogeneity. It is eventually concluded that after optimizing the mechanical and corrosion behaviors as a function of the number of ARB cycles, ARB-processed Zn/Al multilayered composites can be further considered in industrial applications.

Keywords Nanostructured composites, ARB process, Mechanical tensile behaviors, Electrochemical corrosion resistance

1 Introduction

Zinc is widely used in casting processes for making brass alloys and automotive parts. This metal is also utilized in production of printing materials, roofing sheets, biomedical implants, cans for dry cell batteries, and anticorrosion coatings [1]. However, structural applications of pure zinc in industry are limited due to its inadequate mechanical properties (low strength and formability) [2]. Hence, to develop the applications of zinc in industry, its mechanical properties should be improved. There are several methods to improve zinc mechanical performance, as follows: (a) the addition of some alloying elements to pure zinc and fabrication of zinc-based alloys (such as Zn–Mg [3] and Zn–Al alloys [4]), (b) grain refining of zinc via some severe plastic deformation (SPD) methods [5], and (c) fabricating zinc-matrix composites [6]. These processes also affect other properties of zinc, including corrosion properties. Typically, Zn–Al alloys and Zn/Al composites are most commonly used to protect steel structures against corrosion. In this regard, Lee and co-workers [7] fabricated

This is the accepted manuscript (postprint) of the following article:
N. Mosafajahanabad, M. Alizadeh, E. Salahinejad, *Accumulative roll bonding fabrication, tensile and corrosion characterization of Zn/Al multilayered composites*, Archives of Civil and Mechanical Engineering, 22 (2022) 191.
https://doi.org/10.1007/s43452-022-00521-6

Zn–Al alloys and showed that the presence of Al in zinc decreases the corrosion rate compared with pure zinc. They reported that corrosion products enhance the corrosion resistance during corrosion tests in NaCl solutions. In addition, Lu and co-workers [8] fabricated Zn/Al composites and reported that the fabricated composites protect the substrate against corrosion.

The fabrication of Zn/Al composites by cold spraying [8] and powder metallurgy [9] has been previously reported. Among other routes used to produce composites, the use of accumulative roll bonding (ARB) can be beneficially accompanied by producing multilayered composite structures with ultra-fine grains (UFGs) [10]. The development of UFGs can alter some properties, such as mechanical and corrosion behaviors in comparison to their coarse-grained counterparts. In the present work, Zn/6 wt% Al composites were fabricated by this process and some of their structural and mechanical properties were investigated. The other main part of this study was to investigate the corrosion properties of the produced Zn/Al composites in the 3.5 wt% NaCl solution.

2 Experimental procedure

2.1 Materials

Commercially pure Zn and Al sheets with compositions listed in Table 1 were raw materials used in this study. The length and width of the Zn and Al sheets was the same and equal to 200 and 100 mm, respectively, but their thickness was different. The thickness of the Zn and Al sheets was selected to be 0.6 and 0.2 mm, respectively.

This is the accepted manuscript (postprint) of the following article:
N. Mosafajahanabad, M. Alizadeh, E. Salahinejad, *Accumulative roll bonding fabrication, tensile and corrosion characterization of Zn/Al multilayered composites*, Archives of Civil and Mechanical Engineering, 22 (2022) 191.
https://doi.org/10.1007/s43452-022-00521-6

Table 1. Composition of the primary materials used in this research

Sheets	Element (wt%)						
	Zn	Al	Fe	Si	Cu	Mn	Mg
Zn	99.30	0.01	0.32	0.06	0.26	0.01	0.04
Al	0.02	99.42	0.24	0.12	0.12	0.05	0.03

2.2 Fabrication process

The ARB process was used for the fabrication of Zn/Al composites. Zn and Al sheets were degreased with acetone and wire-brushed for surface preparation. To achieve the composition of Zn/6 wt% Al, one Al sheet was placed between two Zn sheets after the surface preparation. The primary sandwich (Zn/Al/Zn) was rolled by a reduction of 66% at room temperature without any lubrication. The reduction of 66% have been used for the creation of appropriate bonding between zinc and aluminum sheets [11]. Afterwards, the rolled sandwich was cut into two equal pieces, degreased with acetone, and scratch-brushed. These specimens were stacked to each other and re-rolled with a draft percentage of 50% reduction. The rolling process was repeated for eight cycles without annealing between each cycle. The rolling speed was 10 rpm, the loading capacity was 20 tons, and the rolls diameter was 20 cm.

This is the accepted manuscript (postprint) of the following article:
N. Mosafajahanabad, M. Alizadeh, E. Salahinejad, *Accumulative roll bonding fabrication, tensile and corrosion characterization of Zn/Al multilayered composites*, Archives of Civil and Mechanical Engineering, 22 (2022) 191.
https://doi.org/10.1007/s43452-022-00521-6

2.3 Structure analysis

X-ray diffraction (XRD, D8 Bruker diffractometer) and scanning electron microscopy (SEM, Tescan Vega 3) were used to evaluate the structure of the composites prepared at various cycles. All of the examinations were done on the perpendicular-transverse plane. X-ray diffraction patterns were recorded in the range of $2\theta = 20–80°$ with the step size and step time of 0.05° and 1 s, respectively. To determine the crystallite size of the produced composite samples, the Williamson–Hall method was also used.

2.4 Tensile testing

Tensile properties of the fabricated composite samples were examined by an Instron tensile test machine according to the ASTME8/E8M-9 standard. The sample preparation was done by a wire cutting machine. The gage length and width of the tensile specimens were 10 mm and 5 mm, respectively. The tensile speed was 0.498 mm/min. After the tensile tests, fracture surfaces were analyzed by SEM.

2.5 Corrosion experiments

Corrosion properties of the Zn/Al composite samples produced at various cycles were investigated in a conventional three-electrode cell. In this cell, the auxiliary electrode was a platinum plate and the reference electrode was Ag/AgCl. The working electrode was the produced composite samples. Using epoxy resin, the composite surfaces were isolated except

This is the accepted manuscript (postprint) of the following article:
N. Mosafajahanabad, M. Alizadeh, E. Salahinejad, *Accumulative roll bonding fabrication, tensile and corrosion characterization of Zn/Al multilayered composites*, Archives of Civil and Mechanical Engineering, 22 (2022) 191.
https://doi.org/10.1007/s43452-022-00521-6

a surface of 1 cm^2 for corrosion exposure from the rolling direction-normal direction plane. Corrosion tests were done by a potentiostat/galvanostat device (Ivium) in the 3.5 wt% NaCl aqueous solution at ambient temperature. Prior to the tests, the composite samples were immersed into the solution for 60 min.

Two methods were used to estimate the corrosion current density (i_{corr}) of the composite samples: (a) Tafel extrapolation and (b) Stern–Geary. In the Tafel extrapolation method, corrosion potential (E_{corr}) and i_{corr} were measured from the intersection of cathodic and anodic Tafel curves. In the Stern–Geary method, i_{corr} was calculated from the following equation [12]:

$$i_{corr} = \frac{b_a \times b_c}{2.303 \times R_p(b_a + b_c)}, \quad (1)$$

where b_a, b_c, and R_p are the anodic Tafel slope, the cathodic Tafel slope, and the linear polarization resistance (LPR), respectively. The Faraday's law was also used to calculate the corrosion rate (R_M) of the fabricated zinc/aluminum composites fabricated at different cycles, as follows [13]:

$$R_M = \frac{M}{nF\rho} i_{corr}, \quad (2)$$

where M is the atomic weight of the matrix (Zn), ρ and n are the density of the metal matrix and the number of electrons exchanged in the corrosion reaction, respectively. F is the Faraday constant which is about 96,500 C/mol.

Electrochemical impedance spectroscopy (EIS) was also done on the composite samples produced at various cycle. The applied AC potential was selected at the range of +5 mV to −5 mV vs. open circuit potential (OCP). The sinusoidal signal amplitude of 10 mV was employed.

This is the accepted manuscript (postprint) of the following article:
N. Mosafajahanabad, M. Alizadeh, E. Salahinejad, *Accumulative roll bonding fabrication, tensile and corrosion characterization of Zn/Al multilayered composites*, Archives of Civil and Mechanical Engineering, 22 (2022) 191.
https://doi.org/10.1007/s43452-022-00521-6

The range of frequency was also selected from 100 mHz to 0.1 MHz. To describe the corrosion behavior of the composite samples fabricated at various cycles, Nyquist and Bode plots were used. *Z*-view software was used for the analysis of the EIS data.

3 Results and discussion

Figure 1 shows the XRD pattern of the zinc–aluminum multilayered composite fabricated by nine ARB cycles. All characteristic diffraction peaks are related to zinc and aluminum, suggesting that no new phases are formed during the ARB process due to the fact that the process is done at room temperature. The temperature of the sample can increase until about 100 °C due to friction between the sample and rolls, but it is not enough to develop a new phase in the composite.

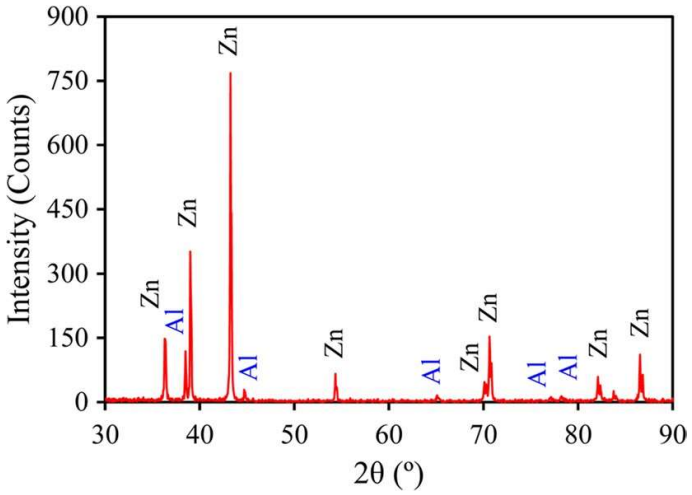

Fig. 1. XRD patterns of the Zn/Al composite sample after the final cycle

This is the accepted manuscript (postprint) of the following article:
N. Mosafajahanabad, M. Alizadeh, E. Salahinejad, *Accumulative roll bonding fabrication, tensile and corrosion characterization of Zn/Al multilayered composites*, Archives of Civil and Mechanical Engineering, 22 (2022) 191.
https://doi.org/10.1007/s43452-022-00521-6

The crystalline size of the composite constituents was determined by the Williamson Hall relation [14]:

$$\beta\cos\theta = \frac{K\lambda}{D} + 4\varepsilon\sin\theta, \tag{3}$$

where θ is the Bragg angle, ε is the lattice strain, λ is the X-ray wavelength, K is a constant (0.9), D is the crystallite size, and β is the width at the half maximum of a diffraction peak. The characteristic peaks of the zinc and aluminum phases in the XRD pattern of the composite after the final ARB cycle were used distinctly to determine the crystalline sizes. Using this formula, the crystallite size of zinc and aluminum was determined to be about 95 and 200 nm, respectively. The difference between the crystallite size of Zn and Al is related to the difference in their stacking fault energy values [15]. It has been reported that the crystallite size of metals with lower stacking fault energy is smaller after the ARB process [16].

The microstructure of the composites fabricated by 1, 5, and 9 ARB cycles is shown in Fig. 2. The number of zinc and Al layers is two and one in the first cycle, and after the ninth cycle they increase to 512 and 256, respectively. In fact, according to Fig. 2c, Al layers with a dark contrast are distributed in the composite after the final ARB cycle. This good distribution of Al layers is due to the increase in the number of the layers by increasing ARB cycles.

This is the accepted manuscript (postprint) of the following article:
N. Mosafajahanabad, M. Alizadeh, E. Salahinejad, *Accumulative roll bonding fabrication, tensile and corrosion characterization of Zn/Al multilayered composites*, Archives of Civil and Mechanical Engineering, 22 (2022) 191.
https://doi.org/10.1007/s43452-022-00521-6

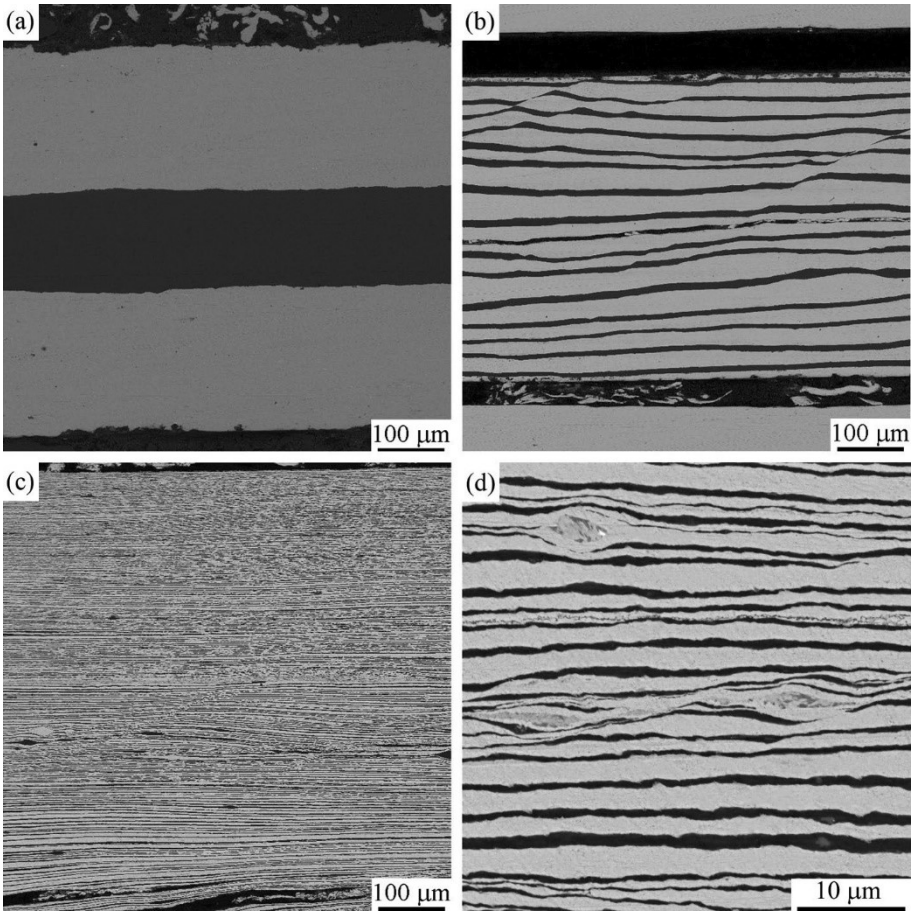

Fig. 2. SEM images of the Zn/ Al composites fabricated by one (**a**), five (**b**), and nine (**c**, **d**) ARB cycles.

This is the accepted manuscript (postprint) of the following article:
N. Mosafajahanabad, M. Alizadeh, E. Salahinejad, *Accumulative roll bonding fabrication, tensile and corrosion characterization of Zn/Al multilayered composites*, Archives of Civil and Mechanical Engineering, 22 (2022) 191.
https://doi.org/10.1007/s43452-022-00521-6

Figure 3a–d shows the SEM micrograph and corresponding elemental maps after the first and ninth cycles. Typically, Zn and Al are distributed homogeneously after the final ARB cycle, whereas both Zn and Al appear as continuous layers at the first cycle (Fig. 3a, b). As can be also seen in Fig. 2, bonding between the two dissimilar constituents of Zn and Al is suitable at different cycles, so that there is no discontinuity between them. Bonding between layers has a basic role in mechanical properties of the fabricated composites. It has been reported that bonding between layers increases by increasing ARB cycles [17].

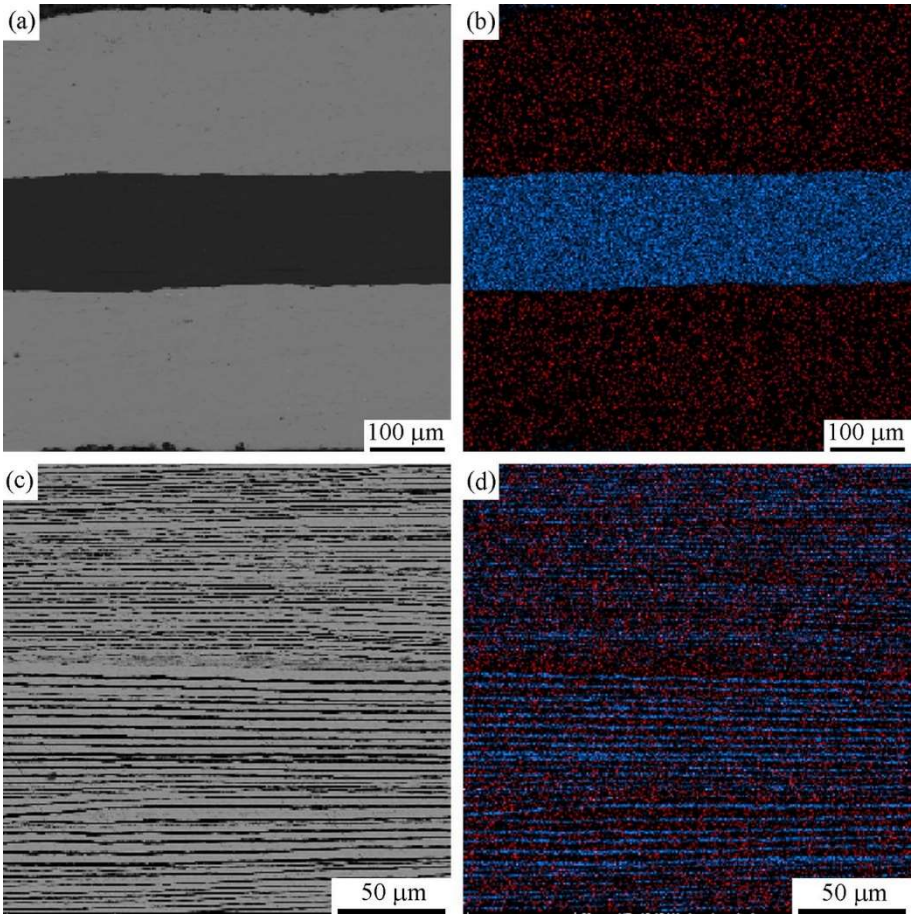

This is the accepted manuscript (postprint) of the following article:
N. Mosafajahanabad, M. Alizadeh, E. Salahinejad, *Accumulative roll bonding fabrication, tensile and corrosion characterization of Zn/Al multilayered composites*, Archives of Civil and Mechanical Engineering, 22 (2022) 191.
https://doi.org/10.1007/s43452-022-00521-6

Fig. 3. SEM image and EDS elemental maps of the Zn/ Al composites fabricated by the first cycle (**a**, **b**) and ninth cycles (**c**, **d**) of ARB. Red and blue contrasts are related to Zn and Al elements, respectively

Figure 4 shows the SEM image and EDS analysis of the samples fabricated by 1 and 9 cycles of ARB. As it can be seen, after one ARB cycle, the interface of Zn and Al is sharp and the slope of the diffusion curves is high (Fig. 4b). After nine ARB cycles, the slope of the diffusion curves in the interface of Zn and Al layers is reduced (Fig. 4d). This suggests that some local intermixing at the interface of Zn and Al layers is created and Zn and Al atoms diffuse into each other. The deformation-induced interdiffusion process is affected by rolling pressure [18], rolling temperature [19], and the type of layers [18]. By increasing the rolling pressure, interdiffusion between layers is increased and bonding can be stronger.

This is the accepted manuscript (postprint) of the following article:
N. Mosafajahanabad, M. Alizadeh, E. Salahinejad, *Accumulative roll bonding fabrication, tensile and corrosion characterization of Zn/Al multilayered composites*, Archives of Civil and Mechanical Engineering, 22 (2022) 191.
https://doi.org/10.1007/s43452-022-00521-6

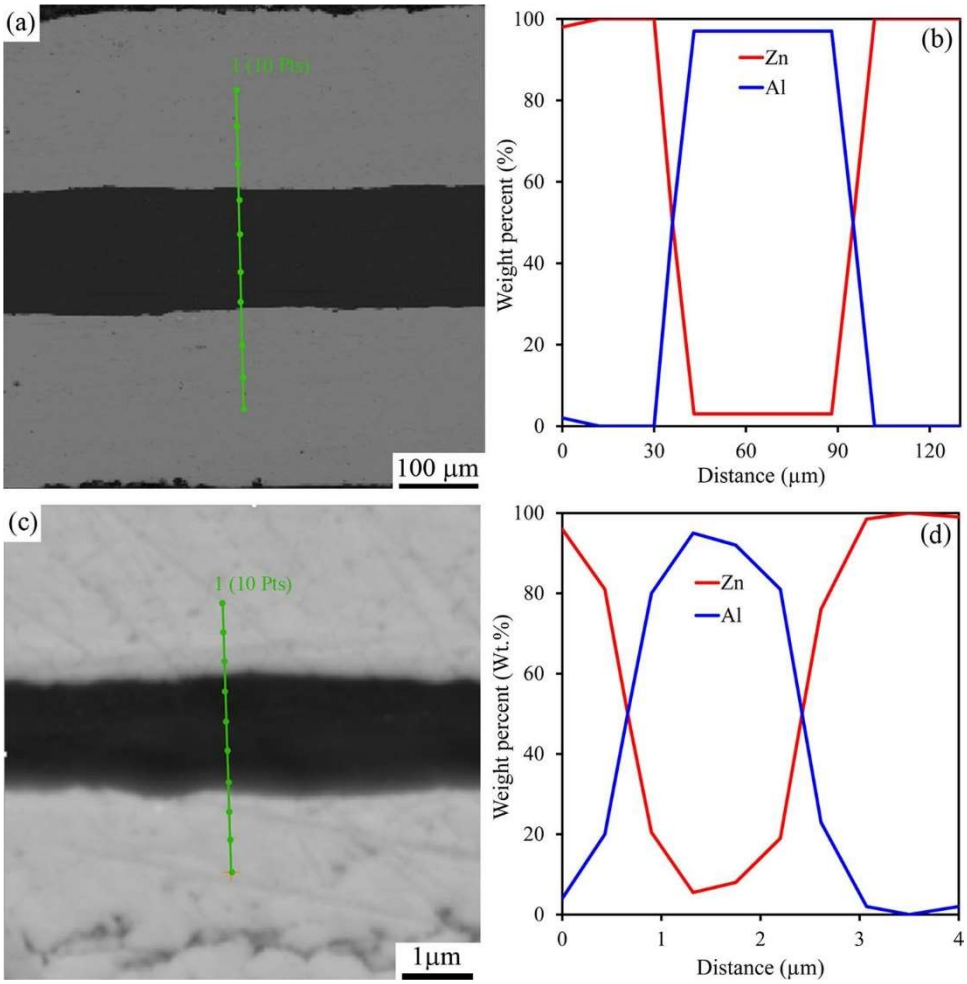

Fig. 4. SEM image and EDS line scan of the Zn/Al composites after the first (**a**, **b**) and ninth (**c**, **d**) cycles of ARB

The engineering stress–engineering strain curves of the Zn/Al-laminated composites fabricated by different ARB cycles and extracted data are shown in Fig. 5. As it can be seen, the strength of the composites first increases and then decreases by progression of the ARB process. In addition, the elongation decreases by increasing the ARB cycles. Plastic instabilities are indeed responsible for this trend. As it can be seen from Fig. 2b and c, some

This is the accepted manuscript (postprint) of the following article:
N. Mosafajahanabad, M. Alizadeh, E. Salahinejad, *Accumulative roll bonding fabrication, tensile and corrosion characterization of Zn/Al multilayered composites*, Archives of Civil and Mechanical Engineering, 22 (2022) 191.
https://doi.org/10.1007/s43452-022-00521-6

phenomena like shear bands, necking, and fracture occur in the microstructure. It has been reported that these plastic instabilities are created due to the difference in the mechanical properties of the composite constituents [16]. The plastic instabilities are affected by the initial thickness, work hardening exponent, and strength coefficient of the constituents [16].

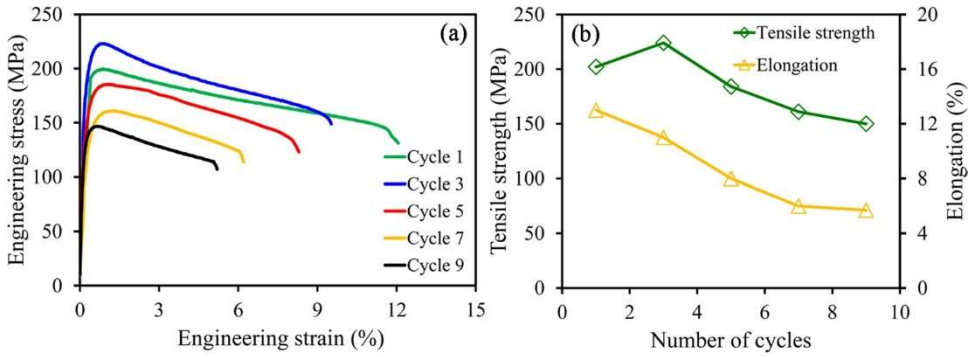

Fig. 5. Engineering stress–engineering strain curves of the Zn/ Al-laminated composites fabricated by different ARB cycles (**a**) and variations of the tensile strength and elongation of the fabricated composites (**b**)

To further evaluate bonding between Zn and Al layers, the tensile fracture surface of the ARBed Zn/Al composites was examined by SEM. Figure 6a shows the fracture surface of the composite fabricated by one cycle. In addition, Fig. 6b and c demonstrates the secondary electron (SE) and back-scattered (BSE) images of the fracture surface of the composite fabricated by five cycles, respectively. In the BSE image of the composite, the Al-rich phase (dark phase) can be clearly distinguished from the Zn-rich matrix. As it can be also seen, there is appropriate bonding between the layers after the tensile test. In addition, it is clear that the fracture mode of the Zn matrix is brittle, where there are no dimples on the fracture surface. In contrast, there are some dimples in the Al layers as indicative of the ductile fracture.

This is the accepted manuscript (postprint) of the following article:
N. Mosafajahanabad, M. Alizadeh, E. Salahinejad, *Accumulative roll bonding fabrication, tensile and corrosion characterization of Zn/Al multilayered composites*, Archives of Civil and Mechanical Engineering, 22 (2022) 191.
https://doi.org/10.1007/s43452-022-00521-6

Comparing the fracture surface of the composites fabricated by one cycle (Fig. 6a) and five cycles (Fig. 6b) shows that by increasing the ARB cycles, dimples are decreased and the fracture mode changes from ductile to brittle.

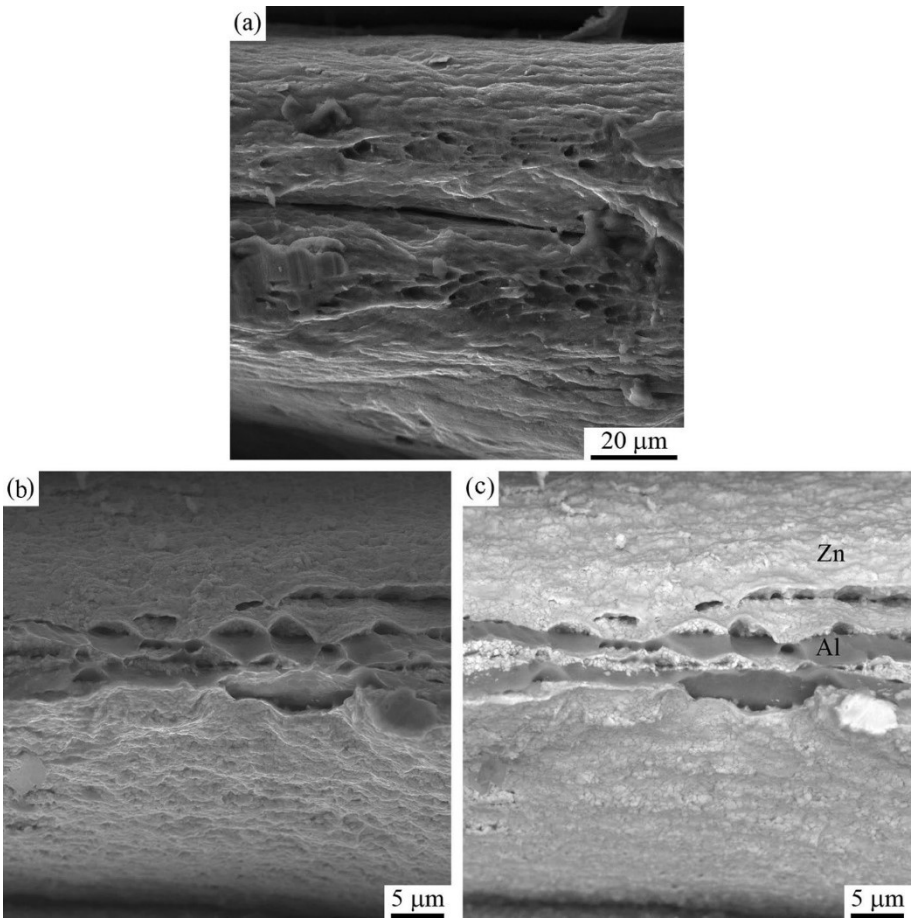

Fig. 6. Tensile fracture surface of the Zn/Al composite after one cycle (**a**) and tensile fracture surface of the Zn/Al composite after five cycles (**b** and **c**): **b** secondary electron image and **c** back-scattered electron image

The potentiodynamic polarization plots of the Zn/Al multilayered composites fabricated at various ARB cycles after stabilization for 60 min in the 3.5 wt% NaCl solution are shown

This is the accepted manuscript (postprint) of the following article:
N. Mosafajahanabad, M. Alizadeh, E. Salahinejad, *Accumulative roll bonding fabrication, tensile and corrosion characterization of Zn/Al multilayered composites*, Archives of Civil and Mechanical Engineering, 22 (2022) 191.
https://doi.org/10.1007/s43452-022-00521-6

in Fig. 7. Table 2 also lists corrosion parameters extracted from the polarization curves. It is obvious that the corrosion tendency is first increased and then decreased by increasing ARB cycles. The corrosion potential of the composite sample after the first ARB cycle is about − 1.1 V vs. Ag/AgCl and it increased to about − 0.95 V after the final cycle. In fact, the decrease in the corrosion tendency is due to the improvement of the microstructure in terms of the elimination of pores and discontinuities between the layers by increasing ARB cycles [20]. By increasing ARB cycles, the corrosion current density is increased after the first cycle and it decreased after the third cycle. It has been reported that the corrosion properties of a metal-matrix composite are affected by the following factors; (1) galvanic corrosion between the composite constituents, (2) the type, geometry, and volume fraction of the reinforcement, (3) the fabrication process of the composite, and (4) the microstructure of the composite [21]. The degree of galvanic corrosion in metal-matrix composites depends on (a) the matrix alloy, (b), the reinforcement electrochemistry, and (c) the environment of corrosion testing. In the fabricated multilayered composites, galvanic corrosion occurs between Zn and Al. However, the difference in the potential of Zn and Al in the 3.5 wt% NaCl solution is low; thus, the degree of galvanic corrosion is low. In addition, reactions between the reinforcement and matrix can create intermetallic phases and intensify galvanic corrosion. In this study, according to the XRD and EDS analyses, no new phase was formed between Zn and Al.

This is the accepted manuscript (postprint) of the following article:
N. Mosafajahanabad, M. Alizadeh, E. Salahinejad, *Accumulative roll bonding fabrication, tensile and corrosion characterization of Zn/Al multilayered composites*, Archives of Civil and Mechanical Engineering, 22 (2022) 191.
https://doi.org/10.1007/s43452-022-00521-6

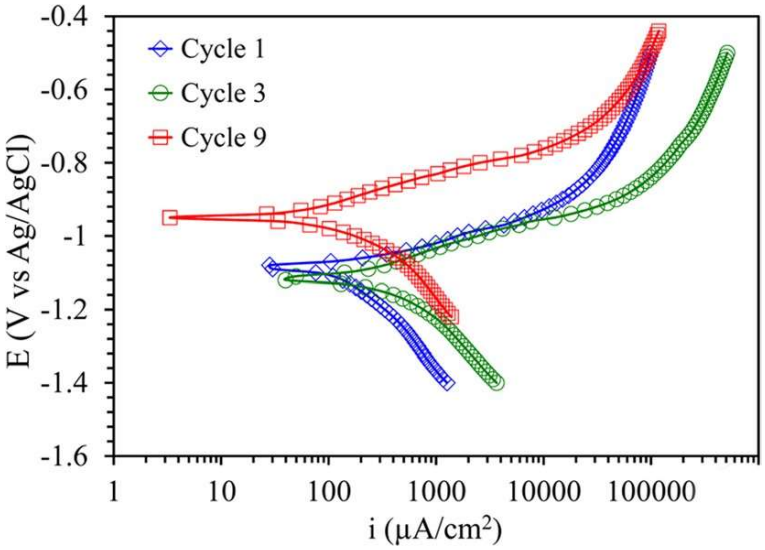

Fig. 7. Polarization curves of the Zn/Al composites fabricated by various ARB cycles

Table 2. Corrosion parameters of the composite samples fabricated by the ARB process

Sample	E_{corr} (V)	Tafel extrapolation method *i*corr (μA/cm²)	Stern–Geary method				
			b_a (mV/dec)	b_c (mV/dec)	*LPR* (Ω)	i_{corr} (μA/cm²)	Corrosion rate (MPY)
Cycles 1	− 1.08	71	58.5	115	2175	78	5.3
Cycles 3	− 1.12	115	74	79.5	1377	121	8.6
Cycles 9	− 0.95	52	80	96.5	3278	58	3.9

Microstructural changes during the fabrication of the Zn/ Al composites by the ARB process play a basic role in the corrosion current density. In the initial cycle of the ARB process, the density of dislocations, lattice strain, and free energy of the structure start to

This is the accepted manuscript (postprint) of the following article:
N. Mosafajahanabad, M. Alizadeh, E. Salahinejad, *Accumulative roll bonding fabrication, tensile and corrosion characterization of Zn/Al multilayered composites*, Archives of Civil and Mechanical Engineering, 22 (2022) 191.
https://doi.org/10.1007/s43452-022-00521-6

increase and thus the microstructure becomes unstable. According to the following equation [22], the value of lattice strain is proportion to the dislocation density:

$$\rho = 14.4\frac{\varepsilon^2}{b^2} \quad (4)$$

where ρ is the dislocation density, ε is the lattice strain, and b is the magnitude of the Burgers vector. In fact, by increasing the dislocation density, the lattice strain is increased. It has been reported that when the dislocation density is increased, the driving force of corrosion reactions is enhanced, which consequently decreases the corrosion resistance [23]. In addition, the lattice strain created due to plastic deformation decreases the activation energy required for the escape of metal atoms to the solution, increasing the corrosion current density [24]. In the present study, the highest dislocation density and lattice strain are related to the composite fabricated by the third cycle. Therefore, it is expected that the corrosion current density is maximum in this sample. By progression of ARB cycles after the third cycle, the density of dislocations and lattice strain are decreased and grain refinement occurs. Low-angle grain boundaries change to high-angle grain boundaries and the microstructure is more stable in comparison to initial cycles. In addition, grain boundaries increase by decreasing the grain size. In this case, grain boundaries act as anodic sites compared to grain interiors because they have a lower corrosion potential [11]. Metallic ions in the form of corrosion products cover the grains; therefore, the anodic reaction and subsequently the corrosion current density are decreased [11]. In addition, during the fabrication of the Zn/Al multilayered composites by the ARB process, the number of layers is increased and the thickness of the layers is decreased. By progression of the ARB process, Al layers as the second phase are distributed in the Zn

This is the accepted manuscript (postprint) of the following article:
N. Mosafajahanabad, M. Alizadeh, E. Salahinejad, *Accumulative roll bonding fabrication, tensile and corrosion characterization of Zn/Al multilayered composites*, Archives of Civil and Mechanical Engineering, 22 (2022) 191.
https://doi.org/10.1007/s43452-022-00521-6

matrix and the microstructure of the composite becomes more homogenous in comparison to initial cycles. In fact, at the final cycles, due to the improved microstructural homogeneity, the formation of corrosion products which protect the composite against corrosion is easer and the corrosion rate is reduced in comparison to the initial cycles. This is compatible with the literature implying the homogeneity in microstructure and small grain sizes have a beneficial effect on the formation of corrosion products and decrease of dissolution during the corrosion process [22].

The EIS study was also done on the produced composites to further investigate the corrosion resistance of the samples. The EIS plots, Bode plots, and EIS equivalent circuit model of the composites fabricated by 1, 3, and 9 cycles are shown in Fig. 8. As it can be seen in Fig. 8a, there are two semicircles in the Nyquist plots of all the fabricated composites. In fact, there is a small semicircle in the high-frequency region and a larger semicircle in the low-frequency zone.

This is the accepted manuscript (postprint) of the following article:
N. Mosafajahanabad, M. Alizadeh, E. Salahinejad, *Accumulative roll bonding fabrication, tensile and corrosion characterization of Zn/Al multilayered composites*, Archives of Civil and Mechanical Engineering, 22 (2022) 191.
https://doi.org/10.1007/s43452-022-00521-6

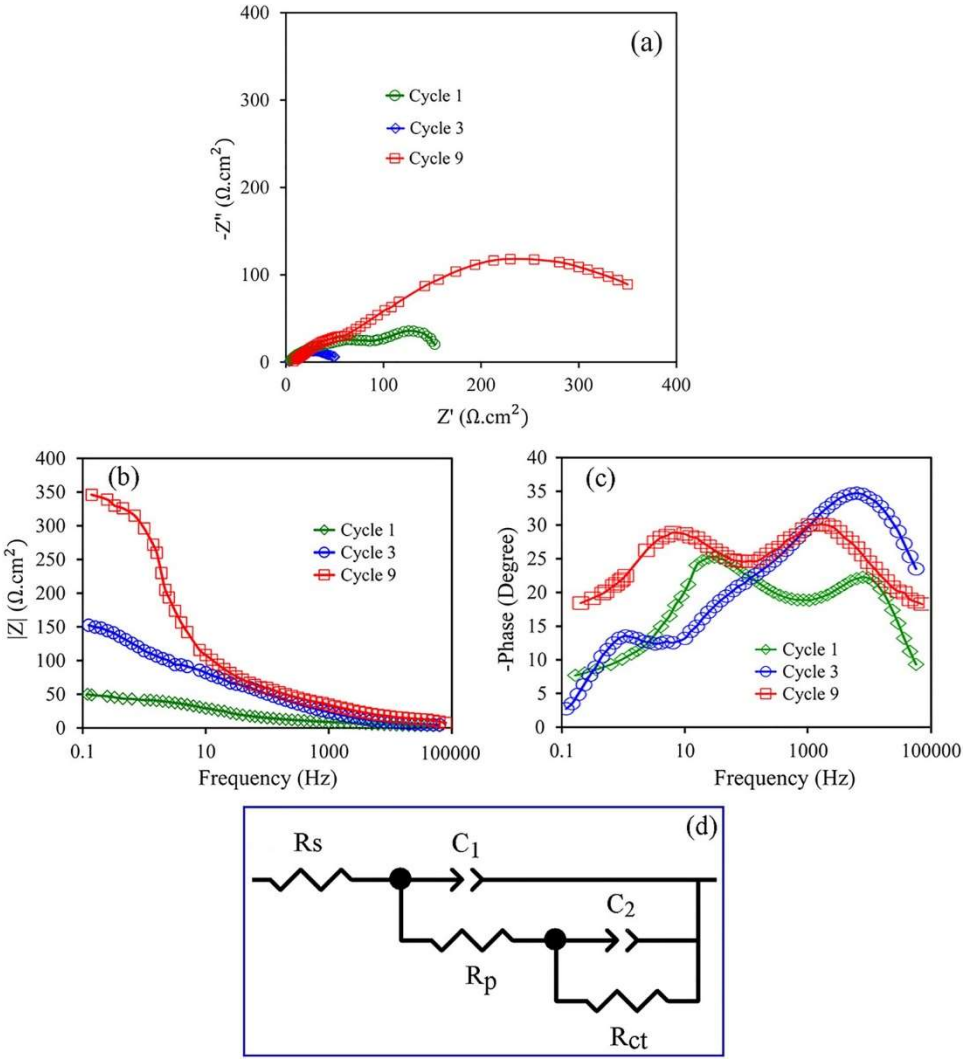

Fig. 8. Nyquist plots (**a**) and Bode plots (**b** and **c**) of the Zn/Al composites produced by various ARB cycles. EIS equivalent circuit model of the produced Zn/Al composites (**d**)

The similarity in the Nyquist plots of all the three composites shows that they present the same corrosion mechanism. The diameter of the semicircles is directly related to the corrosion resistance. Therefore, from Fig. 8a, it is clear that the composite fabricated by three cycles exhibits the minimum corrosion resistance and the composite fabricated by nine cycles

This is the accepted manuscript (postprint) of the following article:
N. Mosafajahanabad, M. Alizadeh, E. Salahinejad, *Accumulative roll bonding fabrication, tensile and corrosion characterization of Zn/Al multilayered composites*, Archives of Civil and Mechanical Engineering, 22 (2022) 191.
https://doi.org/10.1007/s43452-022-00521-6

indicates the maximum. In initial ARB cycles, there are some defects like unbonded areas, pores and discontinuities between the layers. During the corrosion tests in the 3.5 wt% NaCl solution, the penetration of aggressive ions from theses defects increases the dissolution attack. In addition, due to the high density of dislocations and lattice strain, the corrosion resistance is low. At final ARB cycles, most of defects disappear due to the rolling pressure, so that the penetration path of aggressive ions is closed and the corrosion resistance is increased. In addition, at the final ARB cycles, due to the increase of grain boundaries, the value and protection of corrosion products is increased on the surface of the composite samples and hence the corrosion rate decreases. But at the initial ARB cycles, the value of corrosion products is less than that of the final ARB cycles due to the higher grain size.

For comparison, the Bode plot of the produced composite samples is represented in Fig. 8b. It is obvious that the total impedance magnitude for the composite produced by the final ARB cycle is higher than the other composites. This is attributed to the increase of corrosion products which protect the surface of the composite sample against aggressive ions. However, the impedance values of the fabricated composites are low at the low frequency, as shown in Fig. 8b. This is due to the presence of some defects in formed corrosion products [7]. The phase frequency Bode plots of the composites fabricated by different cycles are also shown in Fig. 8c. By increasing the ARB cycles to the final cycle, the phase angle shifts towards higher values due to the increase of the deposition of corrosion products on the composite surface. The corrosion products block active sites and increase the corrosion resistance [7].

Based on the EIS data, the electrical equivalent circuit of the composite samples was plotted (Fig. 8d). R_s, R_{po}, and R_{ct} are the electrolyte resistance, electrolyte resistance inside

This is the accepted manuscript (postprint) of the following article:
N. Mosafajahanabad, M. Alizadeh, E. Salahinejad, *Accumulative roll bonding fabrication, tensile and corrosion characterization of Zn/Al multilayered composites*, Archives of Civil and Mechanical Engineering, 22 (2022) 191.
https://doi.org/10.1007/s43452-022-00521-6

corrosion products defects, and charge transfer resistance at the interface of the composite samples and solution, respectively. C_1 and C_2 are the capacitances of the corrosion products layers and the alloy surface/solution interface, respectively. The calculated equivalent circuit parameters are tabulated in Table 3. The summation of all the ohmic resistances (polarization resistance) for each sample suggests that the composite sample fabricated by the final ARB cycle has the highest corrosion resistance due to the higher uniformity and protection of the deposited corrosion products layer.

Table 3. EIS results of the zinc/ aluminum composites produced by different ARB cycles

Sample	R_s ($\Omega.cm^2$)	R_{po} ($\Omega.cm^2$)	$C1$ ($\Omega^{-1}.cm^{-2}.S^{-n}$)	R_{ct} ($\Omega.cm^2$)	$C2$ ($\Omega-1.\ cm^{-2}.S^{-n}$)
Cycle 1	6.24	226	4.43×10^{-5}	155	5.45×10^{-4}
Cycle 3	6.45	68	6.84×10^{-5}	29	8.25×10^{-4}
Cycle 9	6.65	495	2.52×10^{-5}	224	3.25×10^{-4}

The SEM micrograph of the composite samples produced by different ARB cycles after the corrosion tests is demonstrated in Fig. 9. It is obvious that by increasing ARB cycles, the homogeneity and continuity of corrosion products are increased. Figure 9d typically shows the morphology of corrosion products formed on the composite sample after the ninth cycle at a high magnification. The corrosion products are adherent and have a needle-like morphology. They are uniformly distributed throughout the composite surface and prevent the penetration of the solution towards the composite surface. This morphology has been obtained from a more homogeneous microstructure, lower grain size, and maximum amount of grain

This is the accepted manuscript (postprint) of the following article:
N. Mosafajahanabad, M. Alizadeh, E. Salahinejad, *Accumulative roll bonding fabrication, tensile and corrosion characterization of Zn/Al multilayered composites*, Archives of Civil and Mechanical Engineering, 22 (2022) 191.
https://doi.org/10.1007/s43452-022-00521-6

boundaries associated to the sample prepared by 9 cycles. The SEM image and EDS elemental map taken from the surface of the sample fabricated by 9 cycles are also shown in Fig. 10. The EDS analysis of corrosion products confirms the presence of Zn, Al, O, and Cl. It has been reported that the corrosion products can be oxides, chlorides, and hydroxides of Zn and Al, such as ZnO, Al_2O_3, $Zn(OH)_2$, $Al(OH)_3$, $ZnCl_2$, $AlCl_3$, and $Zn_5(OH)_8Cl_2.H_2O$ (Simonkolleite) [7].

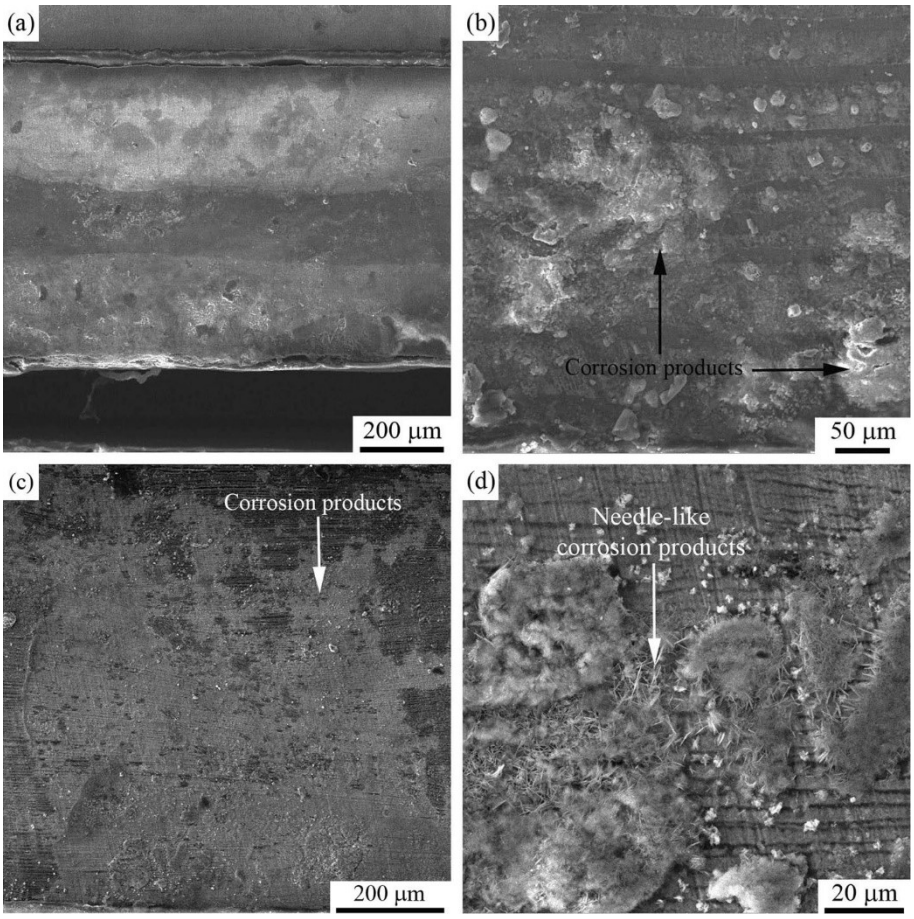

Fig. 9. SEM micrograph of the Zn/Al composites fabricated by **a** 1, **b** 5, and (**c**, **d**) 9 cycles after the corrosion tests in the 3.5% NaCl solution

This is the accepted manuscript (postprint) of the following article:
N. Mosafajahanabad, M. Alizadeh, E. Salahinejad, *Accumulative roll bonding fabrication, tensile and corrosion characterization of Zn/Al multilayered composites*, Archives of Civil and Mechanical Engineering, 22 (2022) 191.
https://doi.org/10.1007/s43452-022-00521-6

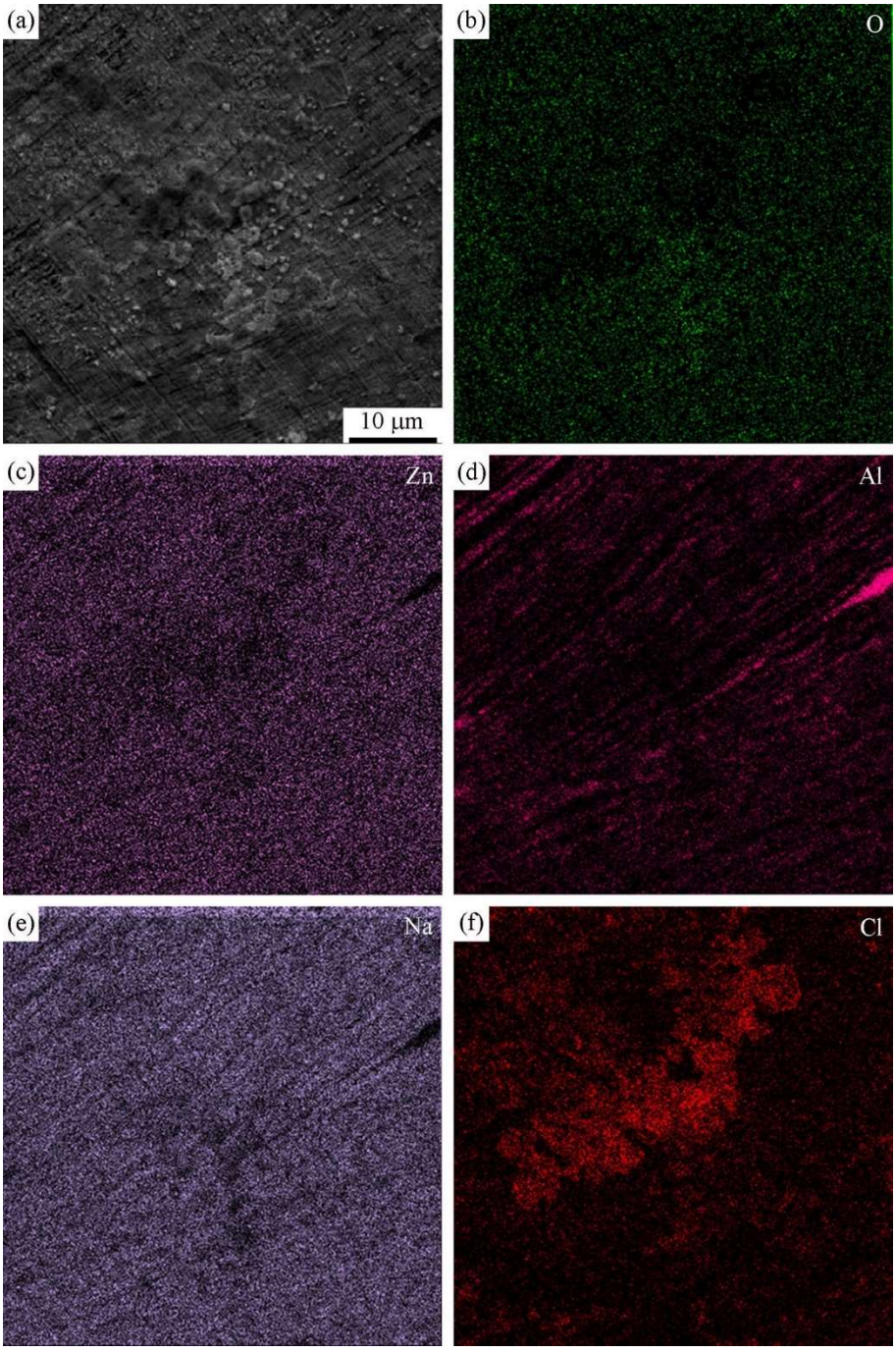

Fig. 10. SEM image and EDS elemental map of the Zn/ Al composite fabricated by 9 cycles after the corrosion test in the 3.5% NaCl solution

This is the accepted manuscript (postprint) of the following article:
N. Mosafajahanabad, M. Alizadeh, E. Salahinejad, *Accumulative roll bonding fabrication, tensile and corrosion characterization of Zn/Al multilayered composites*, Archives of Civil and Mechanical Engineering, 22 (2022) 191.
https://doi.org/10.1007/s43452-022-00521-6

4 Conclusions

In this work, Al layers were incorporated between Zn layers as the second phase, producing Zn/Al multilayered composites by the ARB process. The structural, mechanical tensile, and corrosion properties of the produced composites were investigated and the results are summarized as follows:

1. The crystallite size of the composite constituents was different due to their different stacking fault energy levels. The crystallite size of Zn layers was 95 nm, whereas that of Al layers was about 200 nm at the ninth cycle.
2. Good bonding occurred between Zn and Al layers during the ARB process.
3. Deformation-induced interdiffusion between Zn and Al layers occurred during the ARB fabrication of the composites.
4. The tensile strength of the produced composite samples was controlled by plastic instabilities in the microstructure, so that the maximum strength was achieved in the 3rd cycle.
5. The corrosion tendency deceased by progression of the ARB process due to the elimination of pores and discontinuities between the layers.
6. The corrosion current density increased at initial ARB cycles and then decreased to final cycles due to the effective protection of corrosion products and the decrease of defects.
7. By increasing the ARB cycles and development of the homogeneous microstructure, the homogeneity of corrosion products increased.

This is the accepted manuscript (postprint) of the following article:
N. Mosafajahanabad, M. Alizadeh, E. Salahinejad, *Accumulative roll bonding fabrication, tensile and corrosion characterization of Zn/Al multilayered composites*, Archives of Civil and Mechanical Engineering, 22 (2022) 191. https://doi.org/10.1007/s43452-022-00521-6

References

1. Sahoo SK, Sabat RK, Panda S, Mishra SC, Suwas S. Texture and microstructure evolution of pure zinc during rolling at liquid nitrogen temperature and subsequent annealing. Mater Charact. 2017;123:218–26.

2. Tomov I, Cvetkova C, Velinov V, Riesenkampf A, Pawlik B. Factors influencing the preferential orientations in zinc coatings electrode: posited from chloride baths. J Appl Electrochem. 1989;19:377–82.

3. Huang H, Liu H, Wang LS, Li YH, Agbedor SO, Bai J, Xue F, Jiang JH. A high-strength and biodegradable Zn–Mg alloy with refined ternary eutectic structure processed by ECAP. Acta Metall Sin-Engl. 2020;33:1191–200.

4. Jaglinski T, Lakes RS. Zn–Al-based metal–matrix composites with high stiffness and high viscoelastic damping. J Compos Mater. 2011;46:755–63.

5. Gokhale A, Sarvesha R, Prasad R, Sudhanshu SS, Jain J. A novel approach to refine surface grains in pure zinc using indentation scratch. Mater Lett. 2019;247:151–4.

6. Bobic I, Jovanovic MT, Ilic N. Microstructure and strength of ZA-27-based composites reinforced with Al_2O_3 particles. Mater Lett. 2003;57:1683–8.

7. Lee HS, Kumar singh J, Mohamed Ismail A, Bhattacharya C, Asiful seikh H, Alharthi N, Rizwan Hussain R. Corrosion mechanism and kinetics of Al-Zn coating deposited by arc thermal spraying process in saline solution at prolong exposure periods. Sci Rep. 2019;9:3399.

8. Lu X, Wang S, Xiong T, Wen D, Wang G, Du H. Anticorrosion properties of Zn–Al composite coating prepared by cold spraying. Coatings. 2019;9:210–9.

9. Krystýnová M, Doležal P, Fintová S, Březina M, Zapletal J, Wasserbauer J. Preparation and characterization of zinc materials prepared by powder metallurgy. Metals. 2017;7:396.

10. Alizadeh M, Dashtestaninejad MK. Development of Cu-matrix, Al/Mn-reinforced, multilayered composites by accumulative roll bonding (ARB). J Alloys Compd. 2018;732:674–82.

11. Kalantarrashidi N, Alizadeh M. Structure, wear and corrosion characterizations of Al/20wt% Zn multilayered composites fabricated by cross-accumulative roll bonding. J Manuf Process. 2020;56:1050–8.

12. Wang L, Zhang J, Zeng Z, Lin Y, Hu L, Xue Q. Fabrication of a nanocrystalline NiCo/CoO functionally graded layer with excellent electrochemical corrosion and tribological performance. Nanotechnology. 2006;17:4614–23.

13. Dehgahi S, Amini R, Alizadeh M. Microstructure and corrosion resistance of Ni-Al_2O_3-SiC nanocomposite coatings produced by electrodeposition technique. J Alloys Compd. 2017;692:622–8.

14. Williamson GK, Hall WH. X-ray line broadening from filed aluminium and wolfram. Acta Metall. 1953;1:22–31.

15. Avazzadeh M, Alizadeh M, Tayyebi M. Structural, mechanical and corrosion evaluations of Cu/Zn/Al multilayered composites subjected to CARB process. J Alloys Compd. 2021;867: 158973.

16. Mahdavian M, Ghalandari L, Reihanian M. Accumulative roll bonding of multilayered Cu/Zn/Al: an evaluation of microstructure and mechanical properties. Mater Sci Eng A. 2013;579:99–107.

17. Alizadeh M. Effects of temperature and B_4C content on the bonding properties of roll-bonded aluminum strips. J Mater Sci. 2012;47:4689–95.

18 . Sauvage X, Dinda GP, Wilde G. Non-equilibrium intermixing and phase transformation in severely deformed Al/Ni multilayers. Scripta Mater. 2007;56:181–4.

19. Nasiri Dehsorkhi R, Qods F, Tajally M. Investigation on microstructure and mechanical properties of Al–Zn composite during accumulative roll bonding (ARB) process. Mater Sci Eng A. 2011;530:63–72.

20. Alaneme KK. Corrosion behaviour of heat-treated Al-6063/SiCp composites immersed in 5 wt% NaCl solution. Leonardo J Sci. 2011;18:55–64.

21. Bobic B, Mitrovic S, Babic M, Bobic I. Corrosion of aluminium and zinc-aluminium alloys based metal-matrix composites. Tribol Ind. 2009;31:44–53.

22. Naseri M, Hassani A, Tajally M. Fabrication and characterization of hybrid composite strips with homogeneously dispersed ceramic particles by severe plastic deformation. Ceram Int. 2015;41:3952–60.

23. Vakili M, Borhani E, Ashrafi A. Corrosion behavior of nano-/ ultrafine-grained Al-0.2 wt% Sc alloy produced by accumulative roll bonding (ARB). J Mater Eng Perform. 2018;27:4253–60.

24. Dan S, Ai-bin M, Jing-hua J, Pin-hua L, Dong-hui Y. Corrosion behavior of ultra-fine grained industrial pure Al fabricated by ECAP. Trans Nonferrous Met Soc China. 2009;19:1065–70.